Regular Article - Theoretical Physics

Limits on anomalous top-quark gauge couplings from Tevatron and LHC data

M. Fabbrichesi[1,a], M. Pinamonti[2,b], A. Tonero[3,c]

[1] INFN Trieste, Via Valerio 2, 34127 Trieste, Italy
[2] INFN Trieste gruppo collegato di Udine and SISSA, Via Bonomea 265, 34136 Trieste, Italy
[3] ICTP-SAIFR and IFT UNESP, Rua Dr. Bento Teobaldo Ferraz 271, 01140-070 São Paulo, Brazil

Abstract We review and update current limits on possible anomalous couplings of the top quark to gauge bosons. We consider data from top quark decay (as encoded in the W-boson helicity fractions) and single-top production (in the t-, s- and Wt-channels). We find improved limits with respect to previous results (in most cases of almost one order of magnitude) and extend the analysis to include four-quark operators. We find that new electroweak physics is constrained to live above an energy scale between 430 GeV and 3.2 TeV (depending on the form of its contribution). For comparison, strongly interacting new physics is bounded by scales higher than 1.3 or 1.5 TeV (again depending on its contribution).

1 Motivations and notation

Precision studies of the interaction vertices between the top quark and the gauge bosons provide an important tool in testing the standard model (SM) against new-physics contributions. Currently available measurements from the Tevatron and the LHC already allow one to set stringent limits on possible deviations in the values of these couplings from their SM values. A model independent framework to study these anomalous couplings is provided by effective field theory, where the modifications are encoded into the coefficients of a set of higher dimensional operators that parametrize the effects of new physics at low energy.

The top quark has both strong and electroweak (EW) interactions. While all interactions come together in collider physics, it is possible to separate in most processes the EW from the strong part so that the anomalous vertices can be discussed separately. In this paper we concentrate on the study of the Wtb vertex; the strong interaction $Gt\bar{t}$ vertex was recently studied in [1]—the results of which are here reported. Possible deviations in the interaction between the top quark and the neutral bosons Z and γ—they enter the associated productions $t\bar{t}Z$ and $t\bar{t}\gamma$—are left out because they still are poorly measured.

1.1 Effective Wtb vertex

Following the literature [2], we write the effective lagrangian that describes, after EW symmetry breaking, the most general Wtb vertex as

$$\mathcal{L}_{Wtb} = -\frac{g}{\sqrt{2}}\bar{b}\gamma^\mu(V_L P_L + V_R P_R)t W_\mu^- - \frac{g}{\sqrt{2}}\bar{b}\frac{i\sigma^{\mu\nu}q_\nu}{m_W}$$
$$\times (g_L P_L + g_R P_R)t W_\mu^- + \text{h.c.}, \qquad (1)$$

where g is the $SU(2)_L$ gauge coupling, $P_{L,R}$ the chiral projectors are $(1 \pm \gamma_5)/2$, and $\sigma^{\mu\nu} = i[\gamma^\mu, \gamma^\nu]/2$. The coefficients V_L, V_R, g_L, and g_R are, in general, complex dimensionless constants. In this work we will restrict ourselves to the CP-conserving case and these couplings are taken to be real. In the SM the Wtb vertex in Eq. (1) reduces at the tree level to the Dirac vertex with $V_L = 1$ (after mass diagonalization, $V_L = V_{tb} \simeq 1$) and we take it to be positive. Corrections to V_L, as well as the other non-zero anomalous couplings V_R, g_L, and g_R can be generated by new physics.

If the physics beyond the SM lies at an energy scale Λ that is larger than the EW scale υ, then we can parametrize its effects via higher dimensional operators respecting the SM symmetries in a series suppressed by inverse powers of the scale Λ. The leading contributions arise at dimension six and can be written as an expansion of the local operators $\{\hat{O}_k\}$,

$$\mathcal{L}_{\text{SM}}^{\dim 6} = \sum_k \frac{c_k}{\Lambda^2} \hat{O}_k, \qquad (2)$$

where c_k are dimensionless coefficients.

[a] e-mail: marco@sissa.it

[b] e-mail: michele.pinamonti@gmail.com

[c] e-mails: alberto.tonero@gmail.com; tonero@ift.unesp.br

The complete list of independent dimension six SM effective operators is reported in [3] of which we follow the notation. The subset of operators that contributes to the anomalous couplings in Eq. (1) consists of the following operators:

$$
\begin{aligned}
\hat{O}_{\varphi q}^{(3)} &= (\varphi^\dagger i \overleftrightarrow{D}_\mu^I \varphi)(\bar{q}_L \sigma^I \gamma^\mu q_L), \\
\hat{O}_{\varphi tb} &= i(\tilde{\varphi}^\dagger D_\mu \varphi)(\bar{t}_R \gamma^\mu b_R), \\
\hat{O}_{tW} &= \bar{q}_L \sigma^{\mu\nu} \sigma^I t_R \tilde{\varphi} W_{\mu\nu}^I, \\
\hat{O}_{bW} &= \bar{q}_L \sigma^{\mu\nu} \sigma^I b_R \varphi W_{\mu\nu}^I
\end{aligned}
\tag{3}
$$

where $q^T = (t, b)$, $\tilde{\varphi} = i\sigma^2 \varphi^*$, and $D_\mu \varphi = \partial_\mu \varphi + ig W_\mu^I \frac{\sigma^I}{2} \varphi + ig' Y_\varphi B_\mu \varphi$. After EW symmetry breaking $\varphi = (0, \upsilon + H/\sqrt{2})$, $\upsilon = 246$ GeV, we can express the anomalous couplings in terms of the effective field theory coefficients as follows:

$$
\begin{aligned}
V_L &= V_{tb} + c_{\varphi q}^{(3)} \frac{\upsilon^2}{\Lambda^2} \simeq 1 + c_{\varphi q}^{(3)} \frac{\upsilon^2}{\Lambda^2}, \\
V_R &= \frac{1}{2} c_{\varphi tb} \frac{\upsilon^2}{\Lambda^2}, \\
g_L &= \sqrt{2} c_{bW} \frac{\upsilon^2}{\Lambda^2}, \\
g_R &= \sqrt{2} c_{tW} \frac{\upsilon^2}{\Lambda^2}.
\end{aligned}
\tag{4}
$$

There is another operator that enters in the processes we consider: the four-fermion operator

$$
\hat{O}_{qq'}^{(3)} = \bar{q}_L \gamma^\mu \sigma^I q_L \bar{q}'_L \gamma^\mu \sigma^I q'_L,
\tag{5}
$$

where $q'^T = (u, d)$ and, as before, $q^T = (t, b)$. It does not give a direct contribution to the anomalous couplings but its interplay with the other operators modifies the limits. For this reason it must be included and its effect parametrized by the new coefficient

$$
C_{4f} = c_{qq'}^{(3)} \frac{\upsilon^2}{\Lambda^2},
\tag{6}
$$

which can be further identified by taking $c_{qq'}^{(3)} = 2\pi$ with the usual convention of writing four-quark operators as

$$
\frac{2\pi}{\Lambda^2} \bar{\psi}_L \gamma^\mu \psi_L \bar{\psi}_L \gamma_\mu \psi_L,
\tag{7}
$$

where the coefficient 2π represents the strength of a strongly interacting new-physics sector—the integration of which gives rise to the effective operator.

The effect of these operators on the top-quark EW anomalous couplings can be best studied in two processes: top decay (by means of the W polarizations) and single-top production.

1.2 Effective $Gt\bar{t}$ vertex

The effective vertex for the $Gt\bar{t}$ interactions can be written as

$$
\mathcal{L}_{Gt\bar{t}} = -g_s \bar{t} \left[\gamma^\mu F_1(q^2) + \frac{i\sigma^{\mu\nu} q_\nu}{2m_t} F_2(q^2) \right] G_\mu t,
\tag{8}
$$

where g_s is the strong $SU(3)_C$ coupling constant, $G_\mu = T_A G_\mu^A$ is the gluon field, T_A are the $SU(3)_C$ group generators, q^μ is the momentum carried by the gluon, and t denotes the top-quark field. The interaction in Eq. (8) is the most general one on assuming that the vector-like nature of the gluon–top quark vertex is preserved by the underlying dynamics giving rise to the composite state.

The leading contributions come from the following two higher dimensional operators:

$$
\begin{aligned}
\hat{O}_1 &= g_s \frac{C_1}{m_t^2} \bar{t} \gamma^\mu T_A t D^\nu G_{\mu\nu}^A \quad \text{and} \\
\hat{O}_2 &= g_s \frac{C_2 \upsilon}{2\sqrt{2} m_t^2} \bar{t} \sigma^{\mu\nu} T_A t G_{\mu\nu}^A
\end{aligned}
\tag{9}
$$

where $D^\nu G_{\mu\nu}^A = \partial^\nu G_{\mu\nu}^A + g_s f^A{}_{BC} G^{\nu B} G_{\mu\nu}^C$, $G_{\mu\nu}^A = \partial_\mu G_\nu^A - \partial_\nu G_\mu^A + g_s f^A{}_{BC} G_\mu^B G_\nu^C$ is the gluon field strength tensor, and the $f^A{}_{BC}$ are the $SU(3)_C$ structure constants. In Eq. (9) the operator $\hat{O}_1$ and $\hat{O}_2$ are, respectively, of dimension six and five. We limit ourselves to the CP-conserving case and the dimensionless coefficients C_1 and C_2 are taken to be real. The operator $\hat{O}_1$ gives the leading q^2 dependence to F_1, while $\hat{O}_2$ gives the q^2-independent term of F_2:

$$
F_1(q^2) = 1 + C_1 \frac{q^2}{m_t^2} + \cdots \quad \text{and} \quad F_2(0) = \sqrt{2} C_2 \frac{\upsilon}{m_t}.
\tag{10}
$$

Operators of higher dimensions can in general contribute—they gives further terms in the expansion of the form factors—but their effect is very much suppressed. The form of the coefficients in front of the operators in Eq. (9) is conventional and dictated, in our case, by the analogy with the electromagnetic form factors. In addition, the operator $\hat{O}_2$ is written for convenience with an extra factor υ/m_t because it can be thought of as coming, after EW symmetry breaking, from a dimension six $SU(3)_C \times SU(2)_L \times U(1)_Y$ gauge invariant operator that includes the Higgs boson field.

These vertices were analyzed (most recently in [1] where references to all related works can be found) by means of the $t\bar{t}$ production cross section and spin correlations. The following limits are found:

$$
-0.008 \leq C_1 \leq 0.015 \quad \text{and} \quad -0.023 \leq C_2 \leq 0.020.
\tag{11}
$$

These limits give a direct bound on the magnetic moment μ and the RMS radius $\langle r^2 \rangle$, traditionally used to characterize the size of extended objects. They correspond to

$$\sqrt{\langle r^2 \rangle} < 4.6 \times 10^{-4} \text{ fm} \quad (95\% \text{ CL})$$
$$\text{and} - 0.046 < \mu - 1 < 0.040 \quad (95\% \text{ CL}). \quad (12)$$

We take the coefficients C_1 and C_2 to be zero when studying EW anomalous couplings—they only enter one channel of the single-top production—and assume that the strong interaction of the top quark follows the SM in all production processes.

2 Methods

In order to study the effect of anomalous couplings on top decay rates and single-top production cross sections at the LHC and Tevatron, we first use FEYNRULES [4] to implement our model, which has been defined to be the SM with the addition of the effective operators in Eqs. (3) and (5). The dependence on these operators is encoded in the coefficients $c_i = V_L, V_R, g_L, g_R, C_{4f}$.

FEYNRULES provides the Universal FeynRules Output (UFO) with the Feynman rules of the model. The UFO is then used by MADGRAPH 5 [5] (MG5) to compute the branching ratios in the decay rates and production cross sections, which we denote by $F_{L,0}^{\text{MG5}}$ and σ_{MG5}, respectively.

MG5 computes the square of the amplitude for each single channel. The partonic level result thus obtained can be compared with the partonic experimental cross section that is extracted by the experimental collaborations.

We compute, using MG5, the top-quark decay width and the single-top production cross section varying the values of the anomalous couplings c_i in a range that goes from -2 to 2—except for V_L that is varied only for positive values. These different values of branching ratios $F_{L,0}^{\text{MG5}}(c_i)$ and cross sections $\sigma_{\text{MG5}}(c_i)$ are used to obtain the limits on the coefficients by comparing the MG5 computation with the measured cross sections and helicity fractions at the LHC at the center-of-mass (CM) energies $\sqrt{s} = 7$ and 8, as discussed in the next section. By proceeding in the same way, we have also computed the rate and production cross section at the Tevatron and compared it with the measured cross section at the CM energy $\sqrt{s} = 1.98$ TeV.

Analytical expressions for the amplitudes that we study numerically can be found in [6].

2.1 Statistical analysis

To obtain 95 % confidence level (CL) limits on the coefficients c_i from the production cross sections, we use the quantity $\Delta\sigma_{\text{exp}}$, defined to be the difference between the central value of the measured cross section $\bar{\sigma}_{\text{exp}}$ and the theoretical value of the SM, $\bar{\sigma}_{\text{th}}$:

$$\Delta\sigma_{\text{exp}} = \bar{\sigma}_{\text{exp}} - \bar{\sigma}_{\text{th}}. \quad (13)$$

The uncertainty on $\Delta\sigma_{\text{exp}}$ is given by summing in quadrature the respective uncertainties:

$$\sqrt{(\delta\sigma_{\text{exp}})^2 + (\delta\sigma_{\text{th}})^2}. \quad (14)$$

Using the cross sections $\sigma_{\text{MG5}}(c_i)$ calculated with MG5 we compute the value of the cross section coming from new physics as:

$$\Delta\sigma_{\text{MG5}}(c_i) = \sigma_{\text{MG5}}(c_i) - \sigma_{\text{MG5}}(0). \quad (15)$$

The quantity $\Delta\sigma_{\text{MG5}}(c_i)$ represents the contribution to the cross section coming from the interference between SM leading order and new-physics diagrams as well as terms quadratic in the anomalous couplings.

Values of c_i for which $\Delta\sigma_{\text{MG5}}(c_i)$ is more than two standard deviations from $\Delta\sigma_{\text{exp}}$, namely

$$\Delta\sigma_{\text{MG5}}(c_i) > \Delta\sigma_{\text{exp}} + 2\sqrt{(\delta\sigma_{\text{exp}})^2 + (\delta\sigma_{\text{th}})^2} \quad (16)$$

or

$$\Delta\sigma_{\text{MG5}}(c_i) < \Delta\sigma_{\text{exp}} - 2\sqrt{(\delta\sigma_{\text{exp}})^2 + (\delta\sigma_{\text{th}})^2}, \quad (17)$$

are considered excluded at 95 % CL.

To obtain the limits from the branching ratios in top decay, as measured by the W-boson helicity fractions, a similar procedure is used. The experiments measure the three fractions F_0, F_L, and F_R (see below for the definition). Being extracted from the same data set and from the same observable, these fractions are not independent. F_R is constrained to be equal to $1 - F_0 - F_L$ and is therefore not considered in the limit extraction. In addition, there is a correlation factor ρ different from 0 between the measured values of F_0 and F_L.

The helicity fractions $F_0^{\text{MG5}}(c_i)$ and $F_L^{\text{MG5}}(c_i)$ are computed within MG5, after adjusting for higher order QCD corrections, and compared to the measured values F_0^{exp} and F_L^{exp}. The only uncertainties we consider are the experimental uncertainties δF_0^{exp} and δF_L^{exp}, the theoretical ones being negligible.

To extract the limits, a likelihood function is defined as:

$$L(c_i) \propto e^{-\frac{1}{2(1-\rho^2)}\left[\chi_0^2(c_i) + \chi_L^2(c_i) - 2\rho \cdot \chi_0(c_i) \cdot \chi_L(c_i)\right]}, \quad (18)$$

where

$$\chi_0(c_i) = \frac{F_0^{\text{exp}} - F_0^{\text{MG5}}(c_i)}{\delta F_0} \quad \text{and} \quad \chi_L(c_i) = \frac{F_L^{\text{exp}} - F_L^{\text{MG5}}(c_i)}{\delta F_L}, \quad (19)$$

and the constraint $\int L(c_i) dc_i = 1$ is imposed.

Then the quantity $L^{95\%}$ is defined as

$$\int_{L(c_i)>L^{95\%}} L(c_i)dc_i = 0.95 \qquad (20)$$

and values of c_i for which $L(c_i) > L^{95\%}$ are considered excluded at 95 % CL.

3 Results

Top-quark decay and single-top production are the two processes where we can directly probe the top coupling to the weak bosons.

The Wbt vertex in top-quark decay is best studied by means of the helicity fractions F_0 and F_L defined, respectively, as the ratios between the rates of polarized decay of the top quark into zero and left-handed W bosons and the total decay width. In the SM they are found, neglecting m_b, to be

$$F_0 = \frac{m_t^2}{m_t^2 + 2m_W^2} \simeq 0.7 \quad \text{and} \quad F_L = \frac{2m_W^2}{m_t^2 + 2m_W^2} \simeq 0.3; \qquad (21)$$

the helicity fraction into right-handed W bosons is vanishingly small. These branching ratios receive corrections from the operators $\hat{O}_{tW}$ and $\hat{O}_{bW}$. The SM values at the next-to-next-to-leading order (NNLO) order in QCD are computed in [7,8].

The best current experimental results are given by CMS [9] for data at $\sqrt{s} = 8$ TeV (integrated luminosity 19.6 fb^{-1}) as

$$F_0 = 0.659 \pm 0.015 \,(\text{stat.}) \pm 0.023 \,(\text{syst.})$$
$$F_L = 0.350 \pm 0.010 \,(\text{stat.}) \pm 0.024 \,(\text{syst.}), \qquad (22)$$
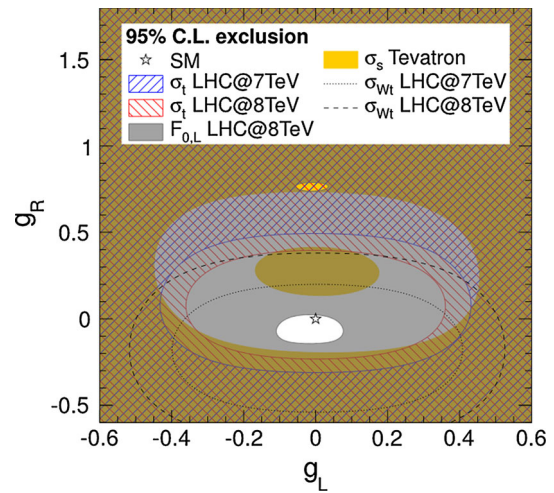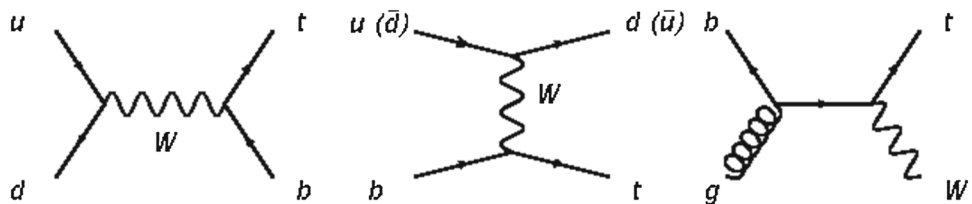
with a correlation coefficient $\rho = 0.95$.

The single-top production occurs through t-, s- and Wt-channel (see Fig. 1). The SM NNLO cross sections have been computed in [10–12], respectively. The corresponding experimental cross sections σ_t, σ_s and σ_{Wt} are available from the LHC and Tevatron data and we utilize the following results (in which the error includes both statistical and systematic contributions):

$$\sigma_t = 67.2 \pm 6.1 \text{ pb} \quad (\text{LHC@7 TeV})[13]$$
$$\sigma_t = 83.6 \pm 7.7 \text{ pb} \quad (\text{LHC@8 TeV})[14], \qquad (23)$$

for single-top production in the t-channel (integrated luminosities of 1.17 and 1.56 fb^{-1} for, respectively, muon and

Fig. 2 95 % CL exclusion limits on the coefficients g_R and g_L ($V_L = 1$, $V_R = C_{4f} = 0$). The *full yellow*, *striped red*, *striped blue*, and *shaded gray areas* indicate the excluded regions from the s- and t-channel production cross sections and from the helicity fractions. *Brown areas* result from the superposition of *yellow* and *gray areas*. The *area* outside the *dashed* (*dotted*) ellipses is excluded by the Wt-channel cross section measurement at the LHC at 8 TeV (7 TeV). The region of allowed values is $-0.109 \leq g_L \leq 0.076$ and $-0.142 \leq g_R \leq 0.024$

electron final states at 7 TeV and 19.7 fb^{-1} at 8 TeV),

$$\sigma_s = 1.29^{+0.26}_{-0.24} \quad (\text{CDF+D0@1.98})[15], \qquad (24)$$

for the s-channel (integrated luminosity 7.5 pb^{-1}) and

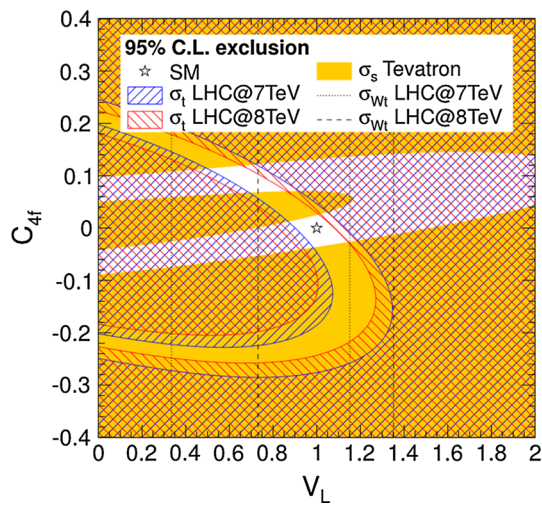$$\sigma_{Wt} = 16^{+5}_{-4} \text{ pb} \quad (\text{LHC@7 TeV})[16]$$
$$\sigma_{Wt} = 25 \pm 4.7 \text{ pb} \quad (\text{LHC@8 TeV})[17], \qquad (25)$$

for the Wt-channel (integrated luminosities 4.9 fb^{-1} at 7 TeV and 12.2 fb^{-1} at 8 TeV).

We study the effect of the operators in Eqs. (3) and (5) by varying the coefficients of two of them at the time and we derive the related limits following the statistical analysis described in the previous section. The results are shown in Figs. 2, 3, and 4.

The determination of the limits on the coefficients g_R and g_L is dominated by the top-quark decay but the single-top production cross section is useful in eliminating larger values (the small area on top of Fig. 2). Accordingly, only the lower region is allowed and

$$-0.109 \leq g_L \leq 0.076 \quad \text{and} \quad -0.142 \leq g_R \leq 0.024. \qquad (26)$$

Fig. 1 Tree-level diagrams for, from *left* to *right*, *s*-, *t*- and *Wt*-channel in top-quark production

Fig. 3 95 % CL exclusion limits on the coefficients C_{4f} and V_L ($g_L = g_R = V_R = 0$). The *full yellow*, *striped red*, *striped blue*, and *shaded gray areas* indicate the excluded regions from the *s*- and *t*-channel production cross sections and from the helicity fractions. The *areas* outside the *dashed (dotted) vertical lines* are excluded by the *Wt*-channel cross-section measurement at the LHC at 8 TeV (7 TeV). The region of allowed values is $0.732 \leq V_L \leq 1.145$ and $-0.037 \leq C_{4f} \leq 0.120$
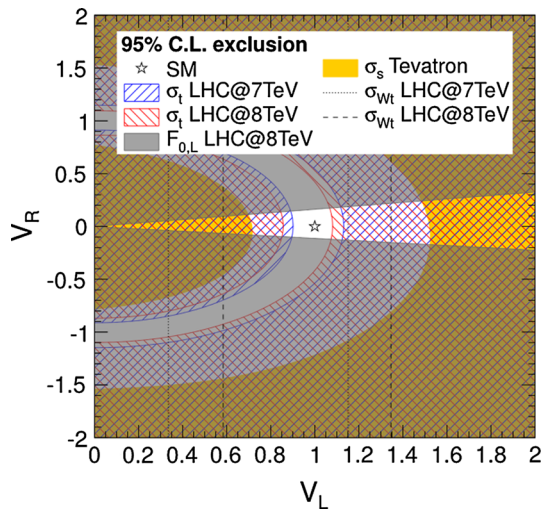
Fig. 4 95 % CL exclusion limits on the coefficients V_R and V_L ($g_L = g_R = C_{4f} = 0$). The *full yellow*, *striped red*, *striped blue*, and *shaded gray areas* indicate the excluded regions from the *s*- and *t*-channel production cross sections and from the helicity fractions. *Brown areas* result from the superposition of *yellow* and *gray areas*. The *areas* outside the *dashed (dotted) vertical lines* are excluded by the *Wt*-channel cross-section measurement at the LHC at 8 TeV (7 TeV). The region of allowed values is $0.891 \leq V_L \leq 1.081$ and $-0.121 \leq V_R \leq 0.173$

The interplay among the various channels of single-top production is crucial in delimiting the allowed region for the parameters C_{4f} and V_L in Fig 3. Unfortunately, the *Wt*-channel is not sensitive to V_R and C_{4f} and the remaining channels are not sufficient in completely delimiting the allowed range of the coefficients to a single region. Accord-

Table 1 Limits (95 % CL) on the coefficients $c_i = V_L, V_R, g_L, g_R, C_{4f}$, and $C_{1,2}$ when they are varied independently of each other and energy scale of the corresponding effective operators

$-0.142 \leq g_R \leq 0.023$	$\lvert g_R \rvert \leq 0.142$, $\Lambda \gtrsim 780$ GeV
$-0.081 \leq g_L \leq 0.049$	$\lvert g_L \rvert \leq 0.081$, $\Lambda \gtrsim 1$ TeV
$0.902 \leq V_L \leq 1.081$	$\lvert V_L - 1 \rvert \leq 0.0099$, $\Lambda \gtrsim 780$ GeV
$-0.112 \leq V_R \leq 0.162$	$\lvert V_R \rvert \leq 0.162$, $\Lambda \gtrsim 430$ GeV
$-0.036 \leq C_{4f} \leq 0.025$	$\lvert C_{4f} \rvert \leq 0.036$, $\Lambda \gtrsim 3.2$ TeV
$-0.008 \leq C_1 \leq 0.015$	$\lvert C_1 \rvert \leq 0.015$, $\Lambda \gtrsim 1.3$ TeV
$-0.023 \leq C_2 \leq 0.020$	$\lvert C_2 \rvert \leq 0.023$, $\Lambda \gtrsim 1.5$ TeV

ingly, the final bound is weakened when both coefficients are allowed to vary simultaneously and we find

$$0.732 \leq V_L \leq 1.145 \quad \text{and} \quad -0.037 \leq C_{4f} \leq 0.120. \quad (27)$$

A future improvement in the *Wt*-channel measurement at the LHC could be instrumental in delimiting the range to a single region.

Finally, it is the interplay between top decay and the *t*-channel of single-top production that provides the limit on the coefficients V_R and V_L (see Fig. 4). We find

$$0.891 \leq V_L \leq 1.081 \quad \text{and} \quad -0.121 \leq V_R \leq 0.173. \quad (28)$$

Notice that all these coefficient are very much constrained by flavor physics. In particular, the coefficient V_R should be [13]

$$-0.0004 \leq V_R \leq 0.0013. \quad (29)$$

When this limit is included, Fig. 4 should be read only along the line $V_R \simeq 0$ with a slightly improved bound

$$0.902 \leq V_L \leq 1.081. \quad (30)$$

Similarly, the coefficient g_L should be approximately less than 0.001 [14,15]. Limits comparable to those from collider physics hold for the other coefficients.

Our results are summarized in Table 1 in the case in which the various anomalous couplings are turned on one at the time.

The limits found can be interpreted in terms of the energy scale of the effective operators in Eq. (3) (see second column of Table 1). By inspection, we see that all EW limits are around 10^{-1} which translates into a characteristic scale $\Lambda \simeq 700$ GeV (actually from 430 GeV to 1 TeV, depending on the contribution) except for the four-quark interaction which has $\Lambda \simeq 3.2$ TeV, if we follow the definition in Eq. (6). Above these limits, there is still room for new physics. These results can be compared with the strong sector interactions of the top quark where the corresponding energy scale is $\Lambda \simeq 1.3$ and 1.5 TeV for, respectively, the operators $\hat{O}_1$ and $\hat{O}_2$ in Eq. (9) [1].
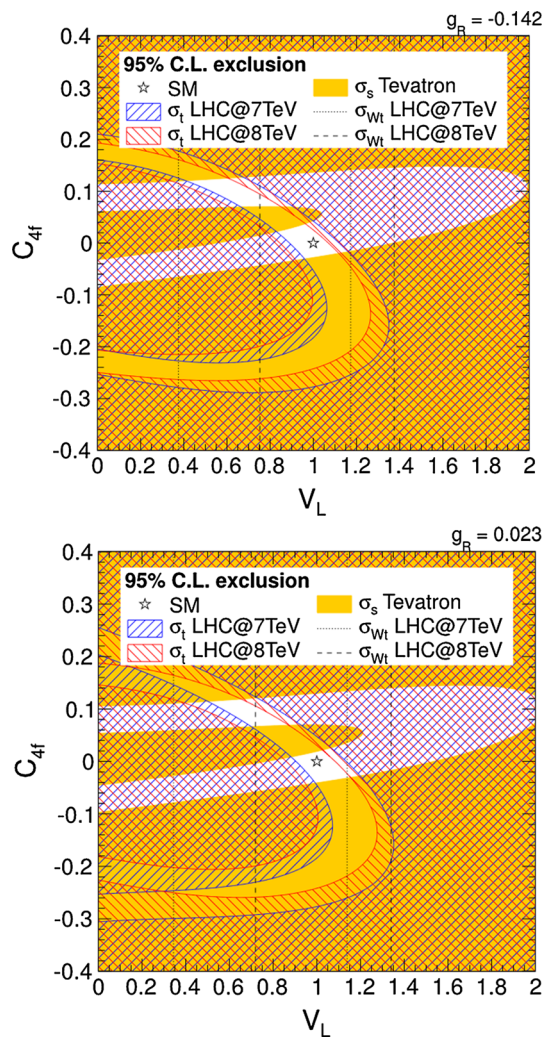
Fig. 5 95 % CL exclusion limits on the coefficients C_{4f} and V_L ($g_L = V_R = 0$) for the two extreme allowed values of the coefficient $g_R = -0.142$ (top) and $g_R = -0.023$ (bottom). The *full yellow*, *striped red*, *striped blue*, and *shaded gray areas* indicate the excluded regions from the *s*- and *t*-channel production cross sections and from the helicity fractions. The *areas* outside the *dashed (dotted) vertical lines* are excluded by the Wt-channel cross-section measurement at the LHC at 8 TeV (7 TeV)

4 Discussion

Constraints on the Wtb vertex from Tevatron and early LHC data were reported in [16]. Future limits for the LHC at 14 TeV were estimated in [17]. The bounds were obtained, as in this paper, by combining the experimental measurements of W-boson helicity fractions and single-top production and by varying two operators at the time. More recently, the measurement of the W-boson helicity fractions has been substantially improved by ATLAS and CMS in [18–20] and limits on the coefficients g_R and g_L were extracted by the experimental collaborations based on these new measurements. Concerning the single-top production, many detailed results have

been released by both Tevatron and LHC experiments [21–25], as reported in the previous section. The improvement is substantial, in most cases of almost one order of magnitude.

We confirm and improve the above limits by means of the most recent data set at 8 TeV by CMS [9] and the combined use of the helicity fractions and single-top production cross sections. The result for the four-fermion operator (5), and its impact on the determination of the coefficient V_L is new.

As expected, the simultaneous presence of more than one anomalous coupling weakens the limits. We have verified that the variation of more than two of the coefficients does not significantly change the result. As an example, in Fig. 5, we show how the limits on the coefficients V_L vs. C_{4f} are changed by taking the two extreme values among those allowed for the coefficient g_R. For $g_R = -0.142$ we have

$$0.753 < V_L < 1.116 \quad \text{and} \quad -0.030 < C_{4f} < 0.094, \quad (31)$$

while for $g_R = 0.023$

$$0.720 < V_L < 1.138 \quad \text{and} \quad -0.041 < C_{4f} < 0.105. \quad (32)$$

These results show that the variation in the value of the limits is around 20 %. Simultaneous variation of other subsets of coefficients, with respect to their limits as taken two at the time, are even smaller. This is explained by the dominance of different processes in the constraints for different pairs of coefficients: helicity fractions in top-quark decay dominate the limits for g_L and g_R while single-top production dominates those of V_L and C_{4f}.

References

1. M. Fabbrichesi, M. Pinamonti, A. Tonero, Stringent limits on top-quark compositeness from top anti-top production at the Tevatron and the LHC. Phys. Rev. D **89**, 074028 (2014). arXiv:1307.5750 [hep-ph]
2. J.A. Aguilar-Saavedra, A minimal set of top anomalous couplings. Nucl. Phys. B **812**, 181 (2009). arXiv:0811.3842 [hep-ph]
3. B. Grzadkowski, M. Iskrzynski, M. Misiak, J. Rosiek, Dimension-six terms in the standard model Lagrangian. JHEP **1010**, 085 (2010). arXiv:1008.4884 [hep-ph]
4. N.D. Christensen, C. Duhr, FeynRules—Feynman rules made easy. Comput. Phys. Commun. **180**, 1614 (2009). arXiv:0806.4194 [hep-ph]
5. J. Alwall et al., MadGraph 5: going beyond. JHEP **1106**, 128 (2011). arXiv:1106.0522 [hep-ph]

6. C. Zhang, S. Willenbrock, Effective-field-theory approach to top-quark production and decay. Phys. Rev. D **83**, 034006 (2011). arXiv:1008.3869 [hep-ph]

7. J. Gao, C.S. Li, H.X. Zhu, Top quark decay at next-to-next-to leading order in QCD. Phys. Rev. Lett. **110**, 042001 (2013). arXiv:1210.2808 [hep-ph]

8. A. Czarnecki, J.G. Korner, J.H. Piclum, Helicity fractions of W bosons from top quark decays at NNLO in QCD. Phys. Rev. D **81**, 111503 (2010). arXiv:1005.2625 [hep-ph]

9. [CMS Collaboration], Measurement of the W-boson helicity in top decays from ttbar production in lepton+jets events at the LHC at sqrt(s)=8 TeV. CMS-PAS-TOP-13-008

10. N. Kidonakis, Next-to-next-to-leading-order collinear and soft gluon corrections for t-channel single top quark production. Phys. Rev. D **83**, 091503 (2011). arXiv:1103.2792 [hep-ph]

11. N. Kidonakis, NNLL resummation for s-channel single top quark production. Phys. Rev. D **81**, 054028 (2010). arXiv:1001.5034 [hep-ph]

12. N. Kidonakis, Next-to-next-to-leading soft-gluon corrections for the top quark cross section and transverse momentum distribution. Phys. Rev. D **82**, 114030 (2010). arXiv:1009.4935 [hep-ph]

13. N. Vignaroli, $\Delta F=1$ constraints on composite Higgs models with LR parity. Phys. Rev. D **86**, 115011 (2012). arXiv:1204.0478 [hep-ph]

14. J. Drobnak, S. Fajfer, J.F. Kamenik, New physics in $t \rightarrow bW$ decay at next-to-leading order in QCD. Phys. Rev. D **82**, 114008 (2010). arXiv:1010.2402 [hep-ph]

15. J. Drobnak, S. Fajfer, J.F. Kamenik, Probing anomalous tWb interactions with rare B decays. Nucl. Phys. B **855**, 82 (2012). arXiv:1109.2357 [hep-ph]

16. J.A. Aguilar-Saavedra, N.F. Castro, A. Onofre, Constraints on the Wtb vertex from early LHC data. Phys. Rev. D **83**, 117301 (2011). arXiv:1105.0117 [hep-ph]

17. F. Bach, T. Ohl, Anomalous top couplings at hadron colliders revisited. Phys. Rev. D **86**, 114026 (2012). arXiv:1209.4564 [hep-ph]

18. [ATLAS Collaboration], Combination of the ATLAS and CMS measurements of the W-boson polarization in top-quark decays. ATLAS-CONF-2013-033

19. S. Chatrchyan et al., [CMS Collaboration], Measurement of the W-boson helicity in top-quark decays from $t\bar{t}$ production in lepton+jets events in pp collisions at $\sqrt{s}$=7 TeV. arXiv:1308.3879 [hep-ex]

20. [CMS Collaboration], Measurement of W-helicity fractions in single top events topology. CMS-PAS-TOP-12-020

21. S. Chatrchyan et al., [CMS Collaboration], Measurement of the single-top-quark t-channel cross section in pp collisions at $\sqrt{s} = 7$ TeV. JHEP **1212**, 035 (2012). arXiv:1209.4533 [hep-ex]

22. V. Khachatryan et al., [CMS Collaboration], Measurement of the t-channel single-top-quark production cross section and of the $|V_{tb}|$ CKM matrix element in pp collisions at $\sqrt{s} = 8$ TeV. arXiv:1403.7366 [hep-ex]

23. T.A. Aaltonen et al., [CDF and D0 Collaborations], Observation of s-channel production of single top quarks at the tevatron. arXiv:1402.5126 [hep-ex]

24. S. Chatrchyan et al., [CMS Collaboration], Evidence for associated production of a single top quark and W boson in pp collisions at $\sqrt{s} = 7$ TeV. Phys. Rev. Lett. **110**, 022003 (2013). arXiv:1209.3489 [hep-ex]

25. [ATLAS and CMS collaborations], Combination of cross-section measurements for associated production of a single top-quark and a W boson at $\sqrt{s} = 8$ TeV with the ATLAS and CMS. ATLAS-CONF-2014-052 and CMS-PAS-TOP-14-009